

Influence of stoichiometry on the dielectric and ferroelectric properties of the tunable (Ba,Sr)TiO₃ ceramics investigated by First Order Reversal Curves method

Liliana Mitoseriu^{a,b,*}, Laurentiu Stoleriu^a, Massimo Viviani^c, Daniele Piazza^d,
Maria Teresa Buscaglia^c, Roberto Calderone^b, Vincenzo Buscaglia^c,
Alexandru Stancu^a, Paolo Nanni^b, Carmen Galassi^d

^a Department of Solid State and Theoretical Physics, Al. I. Cuza University, Blvd. Carol I nr. 11, Iasi 700506, Romania

^b Department of Chemical and Process Engineering, University of Genoa, P.le Kennedy 1, Genoa I-16129, Italy

^c Institute for Energetics & Interphases-CNR, Via de Marini 6, Genoa I-16149, Italy

^d Institute for Science and Technology of Ceramics-CNR, Via Granarolo 64, Faenza I-48018, Italy

Available online 10 March 2006

Abstract

The changes induced by the different stoichiometries in Ba_{0.9}Sr_{0.1}TiO₃ solid solutions, with (Ba,Sr)/Ti = 1 and (Ba,Sr)/Ti > 1, on the dielectric, ferroelectric and ac tunability characteristics are investigated. A small difference in the (Ba,Sr)/Ti ratio causes a shift of the Curie and Curie–Weiss temperatures of 16 and 19 °C, respectively, but does not change the diffuse character of the phase transitions. The FORC method is used for describing the local switching properties and the ac tunability characteristics. Irrespective of the stoichiometry, no clear separation between the reversible and irreversible contributions to the polarization are visible on the FORC diagrams. The maximum of the FORC distribution is located in almost the same position, at low fields, meaning that small fields are necessary to switch the majority of the dipolar units of these systems. The diagram obtained for the solid solutions with (Ba,Sr)/Ti = 1 shrinks towards smaller coercivities in comparison with the Ba-rich samples, due to the smaller Curie temperature, making it closer to the ferro–para phase transition. The tunability determined in the FORC experiment depends not only on the actual field, but also on the reversal field. A dependence of the FORC susceptibility on the two maxima corresponding to the reversal field was found for the stoichiometric samples, while one single maximum at low reversal fields is characteristic of the Ba-rich samples. These results are interpreted in relationship to domain wall mobility, which is higher for the ferroelectric sample, close to its ferro–para phase transition. © 2006 Elsevier Ltd. All rights reserved.

Keywords: Ferroelectric properties; Tunability; BaTiO₃ and titanates

1. Introduction

In the last few years, electric field-tunable dielectrics have attracted much interest for their potential applications as variable capacitors, phase shifters, tunable filters and voltage-controlled oscillators,¹ particularly in circuits and devices needed by the wireless communications industry, for scientific, space, commercial and military use. Among them, SrTiO₃- and BaTiO₃-based solid solutions like (Ba,Sr)TiO₃, (Pb,Sr)TiO₃, Ba(Zr,Ti)O₃, (Ba,Sn)TiO₃ are the most reported materials, due to their high dielectric constant, low losses and high tunability, but also for their low cost, high integrability and poten-

tial for device miniaturisation.^{1–10} Various structures of these materials were studied, as single-crystals,^{1,10} polycrystalline ceramics,^{2,3,9} thick^{4,10} or thin films.^{5–8,10} The electric field-induced tunability describes the ability of a material to change its permittivity by the electric field and is defined as the relative variation of permittivity under the applied field:

$$t(E) = \frac{\varepsilon(0) - \varepsilon(E)}{\varepsilon(0)}, \quad (1)$$

where $\varepsilon(0)$ is the dielectric constant in the absence of a field and $\varepsilon(E)$ is the dielectric constant under the applied field E .

The properties of the solid solution Ba_{1-x}Sr_xTiO₃ (BST) have long been investigated, particularly the relationship between their compositions and microstructural characteristics, with a view to applications in frequency agile microwave circuit

* Corresponding author. Tel.: +40 32 144760; fax: +40 32 213330.
E-mail address: lmtrs@uaic.ro (L. Mitoseriu).

devices.^{1–5,10} Therefore, basic aspects related to tunability are still unclear. For example, in the review of Tagantsev et al.,¹ a few fundamental questions have been formulated and only some of them partially clarified: if the tunability is higher in the ferroelectric phase, in which the spontaneous polarization of the ferroelectric is higher; if there is direct interplay between the dielectric constant ϵ and the tunability $t(E)$; if the high tunability and low losses are contradictory requirements or they can be simultaneously obtained in a given material; how to improve the tunability in films, which is much smaller than in bulk ceramics of the same material; how to define and describe correctly the tunability of one material and its relationship with the microstructural parameters; what is the frequency dependence of $t(E)$ and losses (i.e. to know if good tunability and low losses at low frequencies lead to a high tunability and low losses in the microwave range), etc. In spite of a large volume of publications on the properties of these materials, there is still need for a fundamental approach to describe their tunability and particularly to understand its relationship with composition, microstructures and other parameters (like the electrical and mechanical history and boundary conditions) in particular structures.

The ability of a ferroelectric to change its dielectric constant under an electric field (tunability) is directly related to its non-linear properties, i.e. to the variation of polarization P (and implicitly of the dielectric constant ϵ) with the applied field E . The polarization process of a ferroelectric under an electric field $P(E)$ is a hysteretic phenomenon involving reversible and irreversible domain dynamics, strongly influenced by the composition and microstructures and by external factors such as: temperature, pressure, field amplitude, frequency and phase, field sequence and its history, etc. The non-linear electrical properties of a material can be obtained by different experiments as: by recording of the $P(E)$ hysteresis loops under various types of field sequences, determination of the dependence $\epsilon(E)$ by capacitance measurements, of the $Z(V)$ curves under ac excitation by impedance analysis, by $R(V)$ and $I(V)$ dependences, etc. In addition to the classical methods, the new approach based to the First Order Reversal Curves (FORC) (related to the Preisach model in ferroics^{11,12}), is able to describe the reversible/irreversible (i.e. non-switching/switching) contributions to the polarization and the field-dependence of the differential susceptibilities by using the same experimental data.^{13–17} The experiment involves measurement of minor hysteresis loops between the positive saturation $+E_{\text{sat}}$ and a variable reversal field $E_r \in (-E_{\text{sat}}, +E_{\text{sat}})$ according to the following sequence (as presented in Fig. 1): (i) saturation under a positive field $E \geq +E_{\text{sat}}$; (ii) ramping down to the reversal field E_r , along the descending branch of the major hysteresis loop (MHL); (iii) increasing the field back to $+E_{\text{sat}}$, when P is a function of the fields E and E_r (this is called a FORC curve). The FORC family starting on the descending MHL branch is denoted as $p_{\text{FORC}}^-(E_r, E)$ (Fig. 1) and the differential susceptibilities measured along the FORCs $\chi_{\text{FORC}}^-(E_r, E)$ are given by:

$$\chi_{\text{FORC}}^-(E_r, E) = \frac{\partial p_{\text{FORC}}^-(E_r, E)}{\partial E}. \quad (2)$$

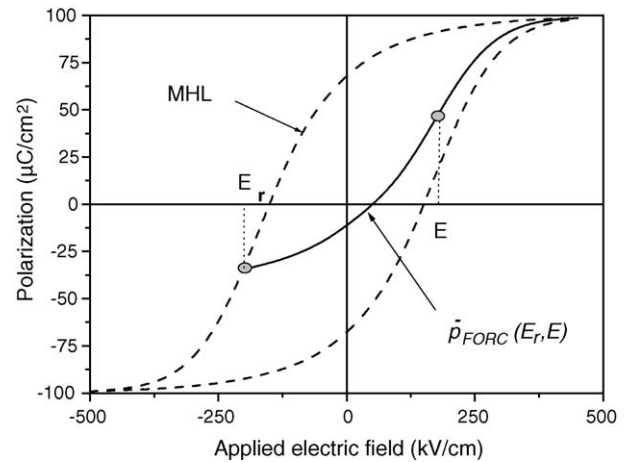
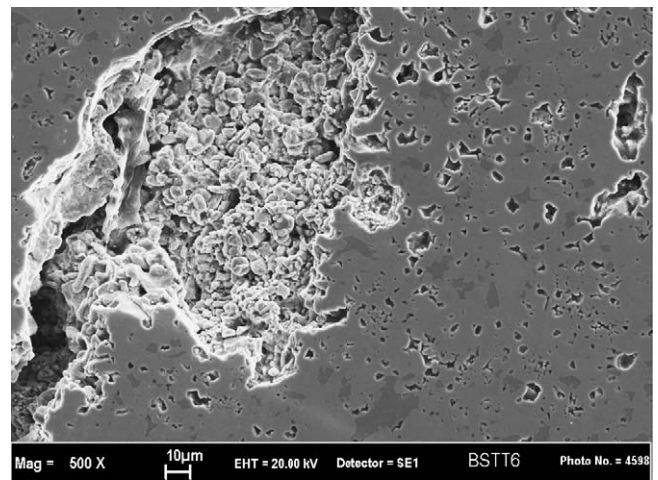
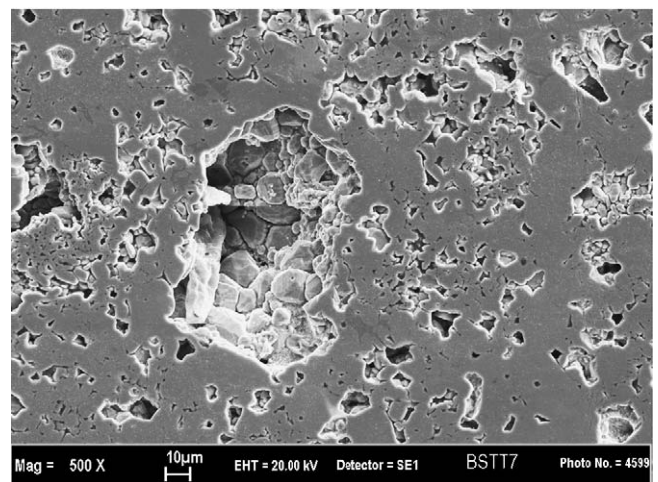


Fig. 1. The definition of the First Order Reversal Curves (FORC) curves $p_{\text{FORC}}^-(E_r, E)$ on a schematic representation of the $P(E)$ hysteresis loop. Dotted line: major hysteresis loop (MHL).



(a)



(b)

Fig. 2. SEM micrographs of the ceramic samples: (a) BST1: (Ba,Sr)/Ti > 1 and (b) BST2: (Ba,Sr)/Ti = 1. Bar = 10 μm .

The FORC diagram represents a contour plot of the FORC distribution, defined as the mixed second derivative of polarization with respect to E and E_r ^{13,18}:

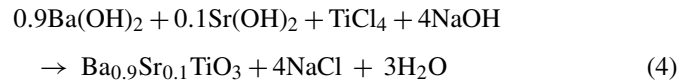
$$\rho^-(E_r, E) = \frac{1}{2} \frac{\partial^2 p_{\text{FORC}}^-(E_r, E)}{\partial E_r \partial E} = \frac{1}{2} \frac{\partial}{\partial E_r} [\chi_{\text{FORC}}^-(E_r, E)] \quad (3)$$

The 3D-distribution $\rho(E_r, E)$ describes the sensitivity of polarization with respect to both the reversal E_r and actual electric field E , while the FORC susceptibility $\chi_{\text{FORC}}^-(E_r, E)$ is related to the ac tunability of the ferroelectric system. By changing the coordinates from (E_r, E) to $\{E_c = (E - E_r)/2, E_i = (E + E_r)/2\}$, the function $\rho(E_c, E_i)$ becomes a distribution of the switchable units over their coercive E_c and bias fields E_i , which is identical

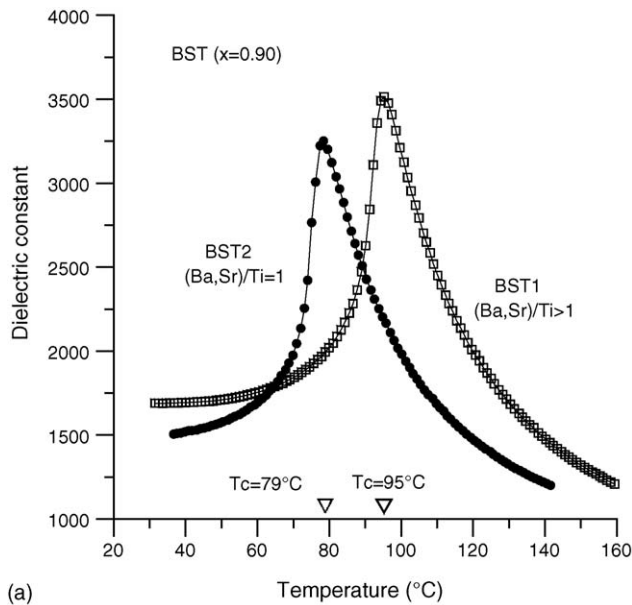
to the Preisach distribution for systems satisfying the requirements of a Classical Preisach model only.^{12,18} In this paper, the FORC method is used to describe the switching and ac tunability characteristics in ceramics of $\text{Ba}_x\text{Sr}_{1-x}\text{TiO}_3$ with $x = 0.90$ having two slightly different nominal (Ba,Sr)/Ti ratios: BST1 with (Ba,Sr)/Ti > 1 and BST2 with (Ba,Sr)/Ti = 1.

2. Ceramic preparation and experiments

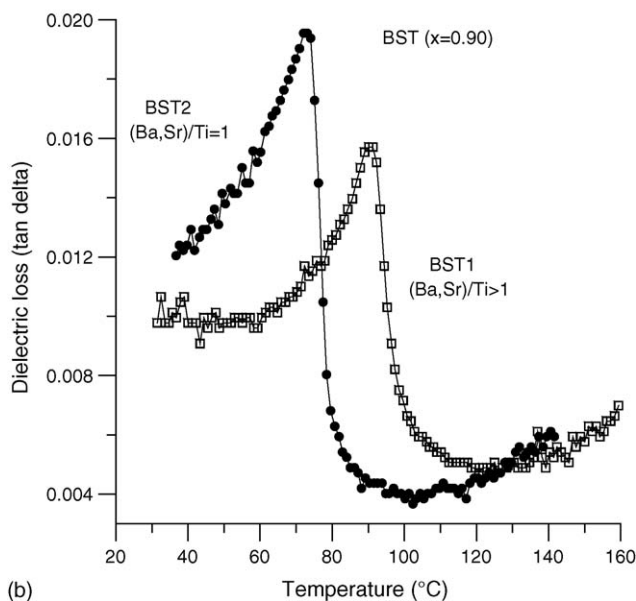
Powders with nominal composition $\text{Ba}_{0.9}\text{Sr}_{0.1}\text{TiO}_3$ were obtained by a modified-low temperature aqueous synthesis (LTAS)¹⁹ performed at 80 °C and atmospheric pressure under inert gas via the reaction:



The resulting powders were washed, dried and calcined in air at 950 °C/2 h, then pressed by cold isostatic pressing at 150 MPa and finally isothermally sintered at temperatures of 1350 °C for 2 h in air. The phase purity was checked by X-ray diffraction (XRD, Co K α radiation, Philips PW1710, Philips, Eindhoven, The Netherlands) and the microstructures examined by scanning electron microscopy (SEM, LEO 1450VP, LEO Electron Microscopy Ltd., Cambridge, UK) of the polished surfaces (without etching). It was previously observed^{19,20} that during the LTAS procedure, the cationic ratio A/B of the ABO₃ perovskite phase is affected by the washing step, mostly through the dissolution of some amount of the A ions from the surface of the particles in water. In order to compensate this depletion, samples with an excess of 2.5 at.% of Ba (denoted as BST1) were also prepared together with the stoichiometric ones (Ba,Sr)/Ti = 1 (denoted as BST2). For the electrical measurements, gold electrodes were sputtered on the polished surfaces of the ceramic samples. An impedance Spectroscopy system (Solartron, SI



(a)



(b)

Fig. 3. The evolution with temperature of the dielectric characteristics of BST1 and BST2 ceramics measured at $f = 1$ Hz: (a) dielectric constant ϵ and (b) dielectric losses ($\tan \delta$).

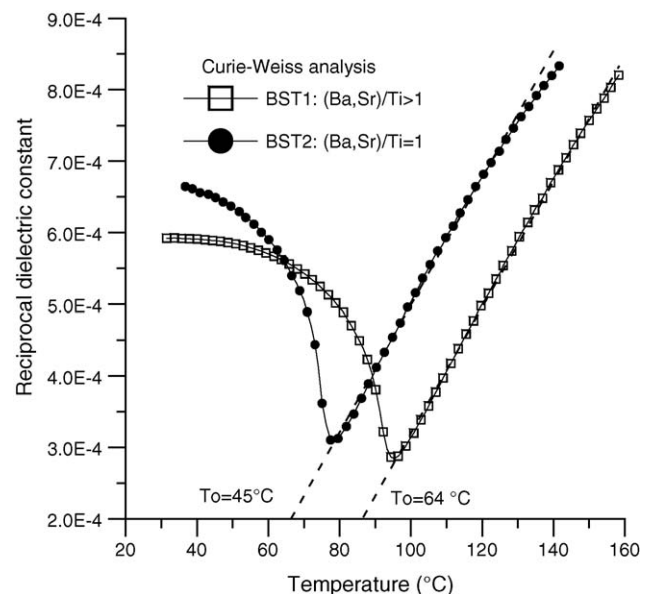


Fig. 4. Curie–Weiss analysis of the dielectric constant data obtained for BST1 and BST2 samples at $f = 1$ Hz.

1260) was used for dielectric characterization in the frequency range $1\text{--}10^6$ Hz and temperatures from 20 to 160 °C, while the $P(E)$ loops and FORC data at room temperature were recorded under a sinusoidal waveform of amplitude $E_0 = 4$ kV/mm and frequency $f = 1$ Hz by using a modified Sawyer–Tower circuit.

3. Results and discussions

The microstructures of the ceramic samples are presented in Fig. 2a and b: (a) for BST1: $(\text{Ba,Sr})/\text{Ti} > 1$ and (b) for BST2: $(\text{Ba,Sr})/\text{Ti} = 1$. The main microstructural characteristics of the two categories of samples are similar, with the exception of the grain size (around $5\ \mu\text{m}$ for BST1 and $>10\ \mu\text{m}$ for BST2). Therefore, the possible grain size influence on the dielectric and ferroelectric properties in this range are negligible,²¹ so that the $(\text{Ba,Sr})/\text{Ti}$ ratio will mainly control the macroscopic properties of the two types of ceramics. The dielectric data and losses

($\tan \delta$) of BST1 and BST2 represented in Fig. 3a and b show indeed a difference in the absolute values (higher dielectric permittivity at room temperature and at the transition point for the sample BST1) and a shift of the Curie temperature T_C of 16 °C, from 79 °C in BST2 to 95 °C in BST1 (Fig. 3a). This behavior is explained by the fact that the Curie temperature T_C of $\text{Ba}_x\text{Sr}_{1-x}\text{TiO}_3$ solid solutions increases with the Ba concentration x (linear in single-crystals and almost linear in the ceramics³) from 75 K at $x = 0.1$ to 395 K for $x = 1$ (BaTiO_3), i.e. with ~ 3.5 K for 1% variation in x . A difference of the Curie–Weiss temperatures of 19 °C is also found: $T_0 = 64$ °C for BST1 and $T_0 = 45$ °C for BST2 (Fig. 4). The Curie–Weiss analysis gave almost the same value for the Curie constant of $C = 1.13 \times 10^5$ K in both samples, meaning that the small difference in the $(\text{Ba,Sr})/\text{Ti}$ ratio does not cause local differences of the electrical properties of the ceramic grain boundaries in the two types of samples, nor any important changes of the ferroelectric

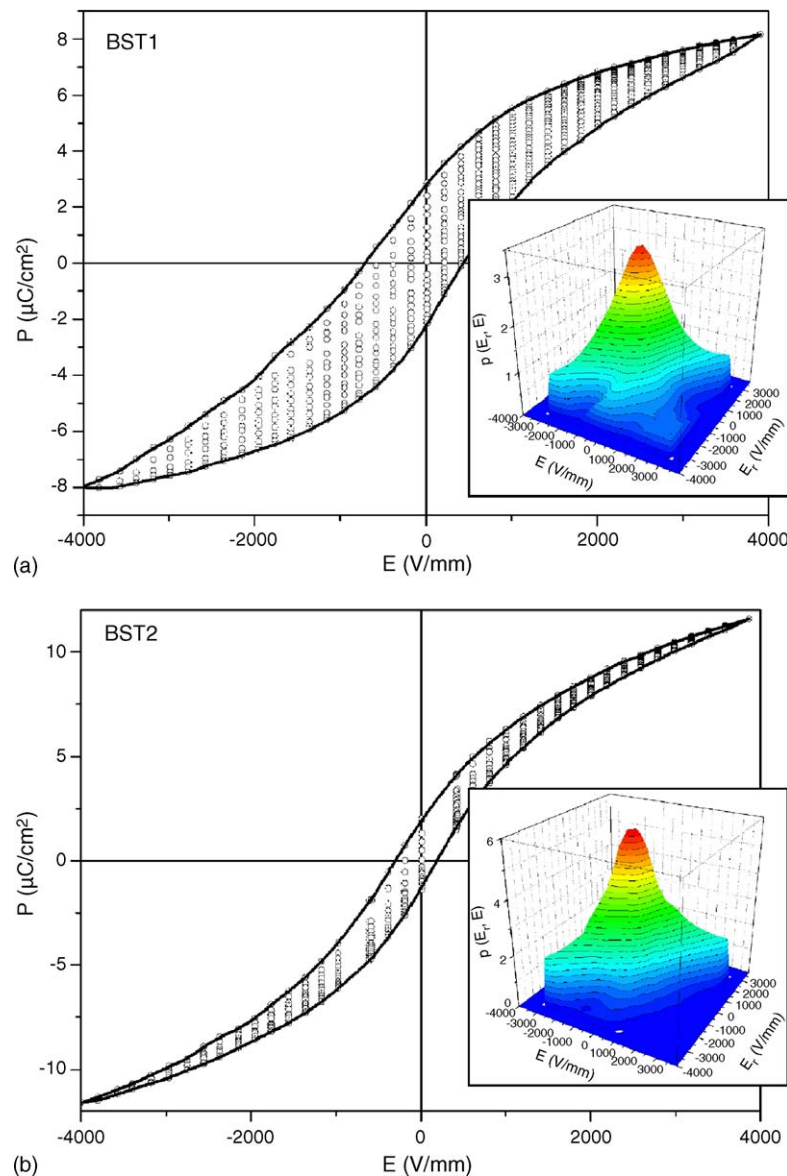


Fig. 5. A family of experimental FORCs $p_{\text{FORC}}^-(E_r, E)$ under a sinusoidal waveform with the amplitude $E_0 = 4$ kV/mm and frequency $f = 1$ Hz obtained for: (a) BST1: $(\text{Ba,Sr})/\text{Ti} > 1$ and (b) BST2: $(\text{Ba,Sr})/\text{Ti} = 1$ ceramic samples at room temperature. The inset corresponds to the 3D-FORC distribution.

dipolar order. In addition, the dielectric constant and losses of both ceramics do not show any dispersion in the investigated range of frequencies 1–10⁶ Hz. The observed diffuse characteristics of the ferro–para phase transition can be described by empirical equations (modified Curie–Weiss laws) as in the case of the ferroelectric relaxors, for example²²:

$$\varepsilon = \frac{\varepsilon_m}{1 + ((T - T_m)/\delta)^\eta}, \quad (5)$$

in which ε_m and T_m correspond to the permittivity peak, δ has a temperature dimension representing the extension interval of the diffuse phase transition and η is a phenomenological parameter equal to 1 in case of ferroelectrics, 2 for full relaxor state and $\eta \in (1, 2)$ for an intermediate character of the diffuse phase transition. For the present samples, the values obtained by fitting are: $\eta = 1.05$, $\delta = 33^\circ\text{C}$ for BST1 and $\eta = 1.02$, $\delta = 34^\circ\text{C}$ for BST2, respectively, showing no change in the extension of the diffuse phase transition and practically full ferroelectric character ($\eta \approx 1$), independent of the (Ba,Sr)/Ti ratio. The dielectric losses are slightly lower for BST1, but generally low for both samples: <1.2% in the ferroelectric state and <2% in the whole range of temperatures (Fig. 3b).

The FORC analysis yields other important information on the BST ceramics. The experimental $P(E)$ MHL loops and FORCs, obtained according to the sequence previously described, are represented in Fig. 5a and b, together with the 3D-FORCs obtained by using the numerical procedure described in Ref. 18. The two FORC distributions look very similar, but some differences are visible on the FORC diagrams (2D-contour plots) in Figs. 6a and b. The $P(E)$ loops are slightly biased ($E_c^- > E_c^+$) and BST1 shows a higher coercivity and slightly lower polarization than BST2. This is due to the fact that at room temperature, BST2 is closer to its ferro–para phase transition than BST1 ceramics. By considering the temperature evolution of the $P(E)$ loops in a ferroelectric material, in which the coercivity and the MHL area are reducing by approaching the ferro–para phase transition, the difference between the two hysteresis loops (Fig. 5) can be understood in terms of difference in the (Ba,Sr)/Ti ratio and from the consequent shift of T_C . The FORC diagrams (Fig. 6) show a small bias for both samples (the maximum of the FORC diagram shifted down towards the bias field, located at $E_i \sim 60\text{ V/mm}$) and overall small coercivity (the maximum of the FORC distribution being located at low values of E_c). The field values corresponding to the maximum of the FORC diagram are low in both ceramics, indicating that rather low fields are needed to overcome the energy barriers for the irreversible domain walls movements. Since there is no net separation of the FORC distribution between the reversible (along the bias axis $E_c = 0$) and the irreversible (for $E_c \neq 0$) components of the polarizations as found for other ferroelectrics, like PZT,^{13,14} it results in a continuous distribution of energy barriers from zero to non-zero values, which are characteristic of this BST composition at room temperature. This is related to the high degree of local compositional inhomogeneity of the solid solutions, giving rise to broad distributed Curie temperatures (having as a consequence the broadening of the phase transition and $\varepsilon(T)$ curves) and broad distributed coercivities (visible on the broad FORC distribu-

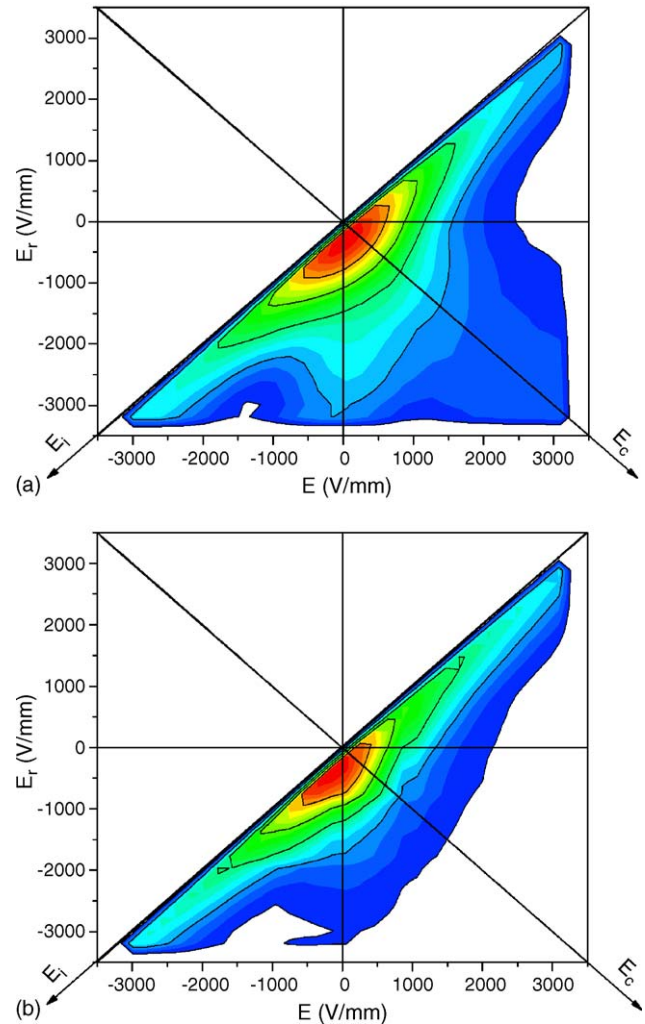


Fig. 6. FORC diagrams calculated for (a) BST1: (Ba,Sr)/Ti > 1 and (b) BST2: (Ba,Sr)/Ti = 1 ceramic samples using the experimental data from Fig. 5.

tions). The main difference between the FORC diagrams of the two compositions is the contraction of the distribution towards lower E_c for the sample BST2 (Fig. 6b) in comparison with BST1 (Fig. 6a), in spite the fact that the position of the peak is almost unchanged. This can be explained by the tendency of the ferroelectric to reduce the energy barriers separating the bi-stable states $\pm P_s$ (i.e. to reduce the local coercivities) while approaching the transition temperature and is a consequence of the stoichiometry difference. In both cases, the FORC diagrams show rather inhomogeneous switching characteristics due to the local variation of composition in the present solid solutions.

Other important information available from the same set of the experimental FORCs is the field dependence of the differential FORC susceptibility related to the ac tunability of the ferroelectric systems. The differential susceptibilities measured along the FORCs $\chi_{\text{FORC}}^-(E_r, E)$ are shown in Fig. 7a and b. It can be seen that the dynamic susceptibilities are functions of both reversal and actual fields (E_r, E). In addition, for a given experiment, the susceptibility is also influenced by the mechanical and electrical history of the sample, this being also valid for static experiments (i.e. for the estimation of the dc tunability).

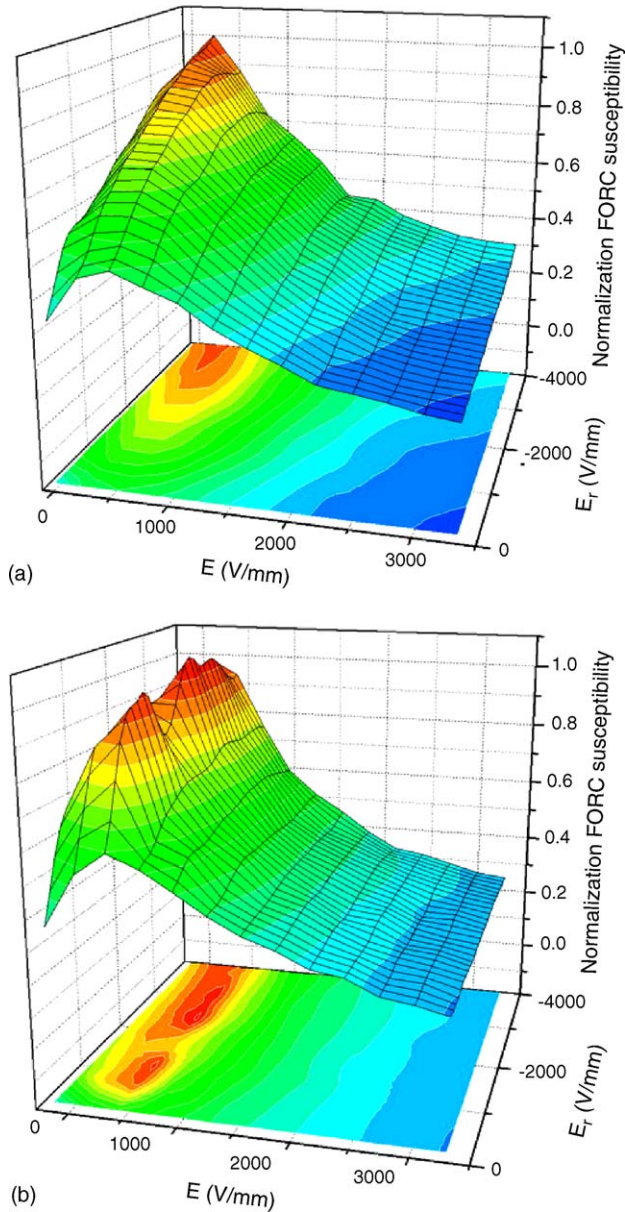


Fig. 7. The normalized distribution of the FORC susceptibilities obtained for (a) BST1: $(\text{Ba,Sr})/\text{Ti} > 1$ and (b) BST2: $(\text{Ba,Sr})/\text{Ti} = 1$ ceramic samples.

It means that a simple definition of tunability given by Eq. (1) is insufficient without defining the experimental conditions and the history of the ferroelectric sample. The maximum tunability is normally obtained along the MHL (i.e. for $E_r = -E_{\text{sat}}$) and for practical reasons this tunability is often used for comparing the performances of various samples. Therefore, in case of the present $\text{Ba}_{0.9}\text{Sr}_{0.1}\text{TiO}_3$ ceramics, this is valid only for the sample BST1 (Fig. 7a), for which the maximum of the FORC susceptibility $\chi_{\text{FORC}}^-(E_r, E)$ is located at $(E_r = -E_{\text{sat}} = -4 \text{ kV/mm}, E \sim 0.3 \text{ kV/mm})$. The tunability of the sample BST2 is not a monotonous function of the reversal field E_r since the FORC susceptibility $\chi_{\text{FORC}}^-(E_r, E)$ diagram has two maxima, located at the same value of $E \sim 0.9 \text{ kV/mm}$, and two different reversal fields E_r : $\sim -1 \text{ kV/mm}$ and $\sim -3 \text{ kV/mm}$. One might take into consideration the possible influence of computational errors pos-

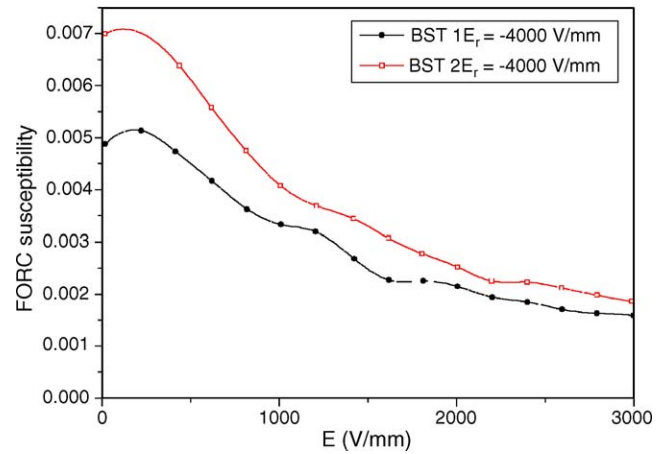


Fig. 8. The FORC susceptibility of the $\text{Ba}_{0.9}\text{Sr}_{0.1}\text{TiO}_3$ ceramics obtained on the major hysteresis loop (for $E_r = -E_{\text{sat}} = -4 \text{ kV/mm}$).

sibly affecting the FORC analysis,¹⁸ particularly in case of the sample BST2 for which a slender $P(E)$ loops was recorded. Therefore, in the authors' opinion, this is excluded since the second derivatives, giving the FORC distributions, show well-defined unique maxima for both samples (Figs. 5–6). Rather, it is possible that the permittivity of the sample BST2 is less homogeneous than that of the sample BST1 due to compositional fluctuations that do not significantly affect the switching characteristics revealed by the FORC diagrams. Therefore, it is impossible at this stage to propose an explanation for this surprising behaviour of the FORC susceptibility of the sample BST2. However, it is clear that the dependence of the dynamic susceptibility of the reversal field might be more complicated than expected; this needs to be carefully investigate. In addition, there is no direct relationship between the switching properties obtained from the FORC distribution and the tunability found from the FORC dynamic susceptibilities.

Finally, a rough comparison of the FORC susceptibilities of BST1 and BST2 samples calculated for $E_r = -E_{\text{sat}} = -4 \text{ kV/mm}$ (Fig. 8) shows that BST2 has a better ability to change its dielectric constant with the applied field (higher tunability), in spite of the fact that this sample has at room temperature lower E_c and permittivity. This can be explained by the effect of reducing the energy barriers for the irreversible domain wall movement together with increasing their mobility while approaching the ferro–para phase transition, giving rise to this difference in their tunabilities. For this reason, there is a tendency to use the ferroelectric materials for tunable elements at temperatures close to their phase transition or even in their paraelectric state, but this leaves other technical problems to be solved.¹ In fact, there is no general agreement concerning the use of materials for tunable applications in the ferroelectric or paraelectric states or close to the ferro–para phase transition. Nevertheless, it is clear that there is no direct relationship between the polarization, coercivity or permittivity and the tunability of the ferroelectric material, as demonstrated for this compositions of BST ceramics. Another important observation is that the ac tunability is not identical to the dc tunability and both of them might result from different experiments on the same sample, because the dynamics of the

domain walls under the applied electrical field can be seriously affected by experimental conditions and sample's history. Thus, the FORC analysis is a very useful instrument for giving indications about the ac tunability in a specific experiment, but its dependence on the dc tunability needs to be further investigated.

4. Conclusions

The dielectric, ferroelectric and tunability properties of the solid solution $\text{Ba}_{0.9}\text{Sr}_{0.1}\text{TiO}_3$ with slightly different stoichiometries, $(\text{Ba,Sr})/\text{Ti} = 1$ and $(\text{Ba,Sr})/\text{Ti} > 1$, are presented. The dielectric constant shows a diffuse ferro–para phase transition with the same degree of diffuseness (temperature extension for the phase transition) due to the variation of the local Curie temperature and ferroelectric character of both ceramics. A shift of the Curie and Curie–Weiss temperatures of 16 and 19 °C, respectively, appears as a consequence of the different $(\text{Ba,Sr})/\text{Ti}$ ratios. The FORC method is used for describing the switching and the ac tunability characteristics of the BST ceramics. The FORC distributions have a diffuse character, indicating a high degree of local compositional inhomogeneity and giving rise to a large distribution in the local interactions and coercive fields. A higher development of the FORCs towards larger coercivities is characteristic of the Ba-rich sample. The maximum is located at rather low fields, independently of the stoichiometry and consequently, no clear separation between the reversible/irreversible contribution to the polarization are visible on the FORC diagrams. The FORC differential susceptibilities, related to the ac tunability, have been estimated from the same set of experimental data. Different behaviour was found for the two samples: a maximum ac tunability on the major hysteresis loop (i.e. for $E_r = -E_{\text{sat}} = -4 \text{ kV/mm}$) for sample BST1 and a more complicated dependence with two maxima at $E \sim -0.9 \text{ kV/mm}$ and $E_r: \sim -1 \text{ kV/mm}$ and $\sim 3 \text{ kV/mm}$, respectively, for BST2. The FORC tunability determined on the major hysteresis loop is sensitive to the stoichiometry, being higher for the sample with the ratio $(\text{Ba,Sr})/\text{Ti} = 1$, that is closer to its ferro–para phase transition. This probably results from a higher mobility of the domain walls when approaching the phase transition than in the ferroelectric state. It was demonstrated that in a dynamic experiment the tunability is dependent on both the actual and reversal fields, thus a correct definition of this characteristic in well-defined conditions has to be used.

Acknowledgements

One of the authors (L.S.) acknowledges the financial support of the COST 525 Action by STMs at ISTECC-CNR Faenza and at the IENI-CNR and University of Genoa, Italy. The present work was also supported by CNCSIS Romanian grants (type A and MATNANTECH).

References

- Tagantsev, A. K., Sherman, V. O., Astafiev, K. F., Venkatesh, J. and Setter, N., Ferroelectric materials for microwave tunable applications. *J. Electroceram.*, 2003, **11**, 5–66.
- Liou, J.-W. and Chiou, B.-S., Effect of direct-current biasing on the dielectric properties of barium strontium titanate. *J. Am. Ceram. Soc.*, 1997, **80**, 3093–3099.
- Vendik, O. G. and Zubko, P., Ferroelectric phase transition and maximum dielectric permittivity of displacement type ferroelectrics $(\text{Ba}_x\text{Sr}_{1-x})\text{TiO}_3$. *J. Appl. Phys.*, 2000, **88**, 5343–5350.
- Su, B. and Button, T. W., The processing and properties of barium strontium titanate thick films for use in frequency agile microwave circuit applications. *J. Eur. Ceram. Soc.*, 2001, **21**, 2587–2795.
- Cole, M. W., Hubbard, C., Ngo, E., Ervin, M., Wood, M. and Geyer, R. G., Structure–property relationships in pure and acceptor-doped $\text{Ba}_{1-x}\text{Sr}_x\text{TiO}_3$ thin films for tunable microwave device applications, 2002, **92**, 475–483.
- Xi, X. X., Li, H.-C., Si, W., Sirenko, A. A., Akimov, I. A., Fox, J. R. et al., Oxide thin films for tunable microwave devices. *J. Electroceram.*, 2003, **4**, 393–405.
- Zhai, J., Yao, X., Shen, J., Zhang, L. and Chen, H., Structural and dielectric properties of $\text{Ba}(\text{Zr}_x\text{Ti}_{1-x})\text{O}_3$ thin films prepared by the sol–gel process. *J. Phys. D: Appl. Phys.*, 2004, **37**, 748–752.
- Xu, J., Menesklo, W. and Ivers-Tiffée, E., Annealing effects on structural and dielectric properties of tunable BZT thin films. *J. Electroceram.*, 2004, **13**, 229–233.
- Wang, T., Chen, X. M. and Zheng, X. H., Dielectric characteristics and tunability of barium stannate titanate ceramics. *J. Electroceram.*, 2003, **11**, 173–178.
- Scott, J. F., Redfern, S. A. T., Zhang, M. and Dawber, M., Polarons, oxygen vacancies, and hydrogen in $\text{Ba}_x\text{Sr}_{1-x}\text{TiO}_3$. *J. Eur. Ceram. Soc.*, 2001, **21**, 1629–1632.
- Preisach, F., Über die magnetische Nachwirkung. *Z. Phys.*, 1935, **94**, 277–302.
- Mayergoyz, I., *Mathematical Models of Hysteresis*. Springer, New York, 1986.
- Stancu, A., Ricinchi, D., Mitoseriu, L., Postolache, P. and Okuyama, M., First-order reversal curves diagrams for the characterization of ferroelectric switching. *Appl. Phys. Lett.*, 2003, **83**, 3767–3769.
- Ricinchi, D., Mitoseriu, L., Stancu, A., Postolache, P. and Okuyama, M., Analysis of the switching characteristics of PZT films by First Order Reversal Curve diagram. *Integr. Ferroelectr.*, 2004, **67**, 103–115.
- Cima, L. and Labouré, E., Characterisation and model of ferroelectrics based on experimental Preisach density. *Rev. Sci. Instrum.*, 2002, **73**, 3546–3552.
- Cima, L. and Labouré, E., A model of ferroelectric behavior based on a complete switching density. *J. Appl. Phys.*, 2004, **95**, 2654–2659.
- Bartic, A. T., Wouters, D. J., Maes, H. E., Rickes, J. T. and Waser, R. M., Preisach model for the simulation of ferroelectric capacitor. *J. Appl. Phys.*, 2001, **89**, 3420–3425.
- Pike, C. R., Roberts, A. P. and Verosub, K. L., Characterizing interactions in fine magnetic particle systems using first order reversal curves. *J. Appl. Phys.*, 1999, **85**, 6660–6667.
- Viviani, M., Nanni, P., Buscaglia, M. T., Leoni, M., Buscaglia, V. and Centurioni, L., Impedance spectroscopy of n-doped $(\text{Ba,Sr})\text{TiO}_3$ ceramics prepared by modified low temperature aqueous synthesis. *J. Eur. Ceram. Soc.*, 1999, **19**, 781–785.
- Nanni, P., Leoni, M. and Buscaglia, V., Low-temperature aqueous preparation of barium metatitanate powders. *J. Eur. Ceram. Soc.*, 1994, **14**, 85–90.
- Akdogan, E. K., Leonard, M. R. and Safari, A., Size effects in ferroelectric ceramics. In *Handbook of Low and High Dielectric Constant Materials and Their Applications*, Vol 2, ed. H. S. Nalwa. Acad. Press, 1999, pp. 61–110.
- Santos, I. A. and Eiras, J. A., Phenomenological description of the diffuse phase transition in ferroelectrics. *J. Phys.: Condens. Matter*, 2001, **13**, 11733–11740.